Observational Study

Medicine®

OPEN

Structural analysis of retinal photoreceptor ellipsoid zone and postreceptor retinal layer associated with visual acuity in patients with retinitis pigmentosa by ganglion cell analysis combined with OCT imaging

Guodong Liu, MD, Hui Li, MD, PhD, Xiaoqiang Liu, MD, PhD, Ding Xu, MD, PhD, Fang Wang, MD, PhD*

Abstract

The aim of this study was to examine changes in photoreceptor ellipsoid zone (EZ) and postreceptor retinal layer in retinitis pigmentosa (RP) patients by ganglion cell analysis (GCA) combined with optical coherence tomography (OCT) imaging to evaluate the structure–function relationships between retinal layer changes and best corrected visual acuity (BCVA). Sixty-eight eyes of 35 patients with RP and 65 eyes of 35 normal controls were analyzed in the study. The average length of EZ was 911.1 ± 208.8 μm in RP patients, which was shortened with the progression of the disease on the OCT images. The average ganglion cell–inner plexiform layer thickness (GCIPLT) was 54.7 ± 18.9 μm in RP patients, while in normal controls it was 85.6 ± 6.8 μm. The GCIPLT in all quarters became significantly thinner along with outer retinal thinning. There was a significantly positive correlation between BCVA and EZ ($r = -0.7622$, $P < 0.001$) and GCIPLT ($r = -0.452$, $P < 0.001$). Therefore, we assess the retinal layer changes from a new perspective in RP patients, which suggests that EZ and GCIPLT obtained by GCA combined with OCT imaging are the direct and valid indicators to diagnosis and predict the pathological process of RP.

Abbreviations: BCVA = best corrected visual acuity, EZ = ellipsoid zone, ERG = electroretinography, ELM = extend limiting membrane, GCIPLT = ganglion cell–inner plexiform layer thickness, GCA = ganglion cell analysis, GCL = ganglion cell layer, IPL = inner plexiform layer, OCT = optical coherence tomography, ORT = outer retinal thickness, RP = retinitis pigmentosa, RNFL = retinal nerve fiber layer, RPE = retinal pigment epithelium, RGC = retinal ganglion cell.

Keywords: best corrected visual acuity, ellipsoid zone, ganglion cell analysis, ganglion cell–inner plexiform layer thickness, optical coherence tomography, retinitis pigmentosa

1. Introduction

Retinitis pigmentosa (RP) is a hereditary degenerative disease of the retina.[1,2] As a cause of visual impairment, the prevalence of RP is about 1 in 4000,[3,4] which is characterized by slowly progressive, concentric constriction of the visual field.[2,5] The earliest histopathological changes in all forms of RP involve shortening of the photoreceptor segments, so there are a number of studies about outer retinal changes,[5–9] while relatively fewer articles about inner retinal thickness.[10,11] In addition, the results showed that the inner retinal layers were preserved or even thickening compared to the outer retinal layers, which was associated with neuronal–glial remodeling, especially in early stage of RP patients.[12] In addition, the morphometry study showed that the ganglion cell number was not statistically different in the various stages of RP.[13] Therefore, currently proposed strategies to treat RP are based on the assumption that the inner retinal cells are intact.[2] However, there were also articles reported less ganglion cells in RP patients than in normal controls.[14,15] Besides, the inner retinal layers including the inner limiting membrane, retinal nerve fiber layer (RNFL), ganglion cell layer (GCL), inner plexiform layer (IPL), and inner nuclear layer measured by manual methods were widely different in previous studies,[11,12,15,16] and RNFL thickness is dramatically different in individuals.[17] So, the general conclusion that the inner retinal cells are intact need to be reassessed, especially by the modern devices.

Ganglion cell IPL (GCIPL), which is topographically less variable among normal individuals, reflects both the retinal ganglion cell (RGC) bodies and the dendrites originating from the macular region. It has been confirmed to be valuable for diagnosing glaucoma obtained by ganglion cell analysis (GCA) incorporate into the new optical coherence tomography (OCT) device, which reflects localized RNFL defects better than

Editor: Stela Vujosevic.

GL and HL have contributed equally to the article.

Authorship: All authors involved in study design, data analysis, and revising of the manuscript, the authors agreed the submission of the article.

Funding/support: The work was supported by the National Natural Science Foundation of China grants (81271029 and 81300772), Specialized Research Fund Q2 for the Doctoral Program of Higher Education (20130072120053), and the Science and Technology Commission of Shanghai Q3 (11Jc1409900).

The authors have no conflicts of interest to disclose.

Supplemental Digital Content is available for this article.

Department of Ophthalmology, Shanghai Tenth People's Hospital Affiliated with Tongji University School of Medicine, Shanghai, PR China.

* Correspondence: Fang Wang, Department of Ophthalmology, Shanghai Tenth People's Hospital Affiliated with Tongji University School of Medicine, 301 Middle Yan Chang Road, Shanghai 200072, PR China (e-mail: milwang_122@msn.com)

Medicine (2016) 95:52(e5785)

Received: 31 August 2016 / Received in final form: 30 November 2016 / Accepted: 1 December 2016

http://dx.doi.org/10.1097/MD.0000000000005785

papillary RNFL in advanced glaucoma.[18,19] However, there is no article to study about GCIPL changes in RP patients by GCA, and the thickness in the previous studies was measured from 2 or 4 points by manual[20,21]; therefore, it is necessary to reconfirm the condition of ganglion cells in RP. Visual function in RP cases was proved to be related with morphological changes of the photoreceptors in the macular area.[22–25] Unfortunately, the analysis of the relationship between GCIPL thickness (GCIPLT) and visual function has not been investigated. With the advent of higher resolution spectral domain (Cirrus high-definition 5000, Carl Zeiss Meditec, Inc.; Dublin, CA) OCT, combined with more precise segmentation of the retinal layers, GCIPLT measurement has become possible.[26] Therefore, it is necessary to use GCA to assess the morphological changes and thickness of GCIPL in RP patients.

In the present study, we use the modern OCT with an axial resolution of 5 μm to evaluate the changes in receptor ellipsoid zone (EZ) and postreceptor retinal layer (GCIPL) in patients with RP. The relationship between best corrected visual acuity (BCVA) and EZ, and GCIPLT were investigated using a linear regression model. The factors affecting visual acuity were further analyzed by multiple linear regressions.

2. Materials and methods

2.1. Materials

In this study, 70 eyes of 35 patients (11 female, 24 male; age range 29–76 years; median age 51.5 years) with a clinical diagnosis of RP were examined, and the average diagnostic duration was 32 ± 6.5 years. Sixty-five eyes of 35 patients (11 female, 24 male; age range 26–78 years; median age 51.8 years) without retinal disease served as normal controls. The study was conducted at Shanghai Tenth People's Hospital between December 2012 and April 2015. The study was conducted in accordance with the tenets of the Declaration of Helsinki. Data collection and analysis were approved by the hospital ethics committee, and informed consent was obtained from all participants. RP patients were diagnosed based on clinical history, funduscopic appearance, visual field testing, and full-field electroretinogram records. All participants underwent a complete ophthalmologic examination, including measurement of BCVA, noncontact tonometry, slit-lamp biomicroscopy, indirect ophthalmoscopy, color fundus photography, full-field electroretinography (ERG), central visual field, and spectral-domain OCT. BCVA, expressed as the logarithm of the minimum angle of resolution (log MAR), finger count, hand movement, light perception, and no light perception were designated as 2, 3, 4, and 5, respectively. All participants followed the selection criteria: ERG was markedly reduced or had no rod response, and the area of central visual field was lost severely. Although some eyes were with good BCVA, the central visual field defect was severe (mean deviation <-20 dB by Octopus Field Analyzer (Haag-Streit, Koeniz, Switzerland)), and the retinal atrophy of the eyes was severely shown by the fundus images.

2.2. Optical coherence tomography evaluation

High-definition (HD)-OCT (Cirrus high-definition 5000 OCT) with an axial resolution of 5 μm was performed on all 70 eyes with RP and 65 eyes of the normal controls. Cross-section images of 6 mm horizontal and vertical scans through the central fovea were obtained. A macular cube 512×128 scan was obtained by Cirrus HD-OCT to obtain the central fovea thicknesses (CFT) and GCIPLT data. The macula thickness and the outer rings, bounded by 3 and 6 mm concentric circles, were constructed using the automated software algorithm. Central subfield thickness was defined as the average thickness in the central 1 mm subfield centered on the fovea. Average macular thickness, foveal thickness, outer macular (superior, nasal, inferior, and temporal) thicknesses, and macular volume were obtained for each eye. The GCA algorithm was incorporated into the newer Cirrus OCT software version 6.5 with the annulus of inner vertical and horizontal diameters of 1 and 1.2 mm, respectively, and outer vertical and horizontal diameters of 4 and 4.8 mm, respectively. As reported,[27] the outer ring size includes the area where the GCL is thickest in a healthy eye. The GCA algorithm identifies the outer boundaries of RNFL and IPL, between which is the GCIPL layer. GCIPLT will be analyzed according to 8 parameters—average, minimum, and 6 sectors (superonasal, superior, superotemporal, inferotemporal, inferior, and inferonasal)—by the GCA algorithm embedded in Cirrus OCT. Grayscale images were used for a more precise identification and measurement of the EZ. Length was measured in the horizontal and vertical scans, and an average value was obtained. Outer retinal thickness (ORT) was defined as the region from the outer plexiform layer to the retinal pigment epithelium (RPE) layer/Bruch complex, consisting of the outer plexiform layer, outer nuclear layer, extend limiting membrane (ELM), myoid zone, EZ, interdigitation zone, and RPE/Bruch complex. ORT was measured 1 mm from the fovea in the horizontal and vertical scans, and an average value was obtained.

To measure RNFL thickness, 200×200 axial scans were used in a $6 \times 6\,mm^2$ area around the optic disc cube. The software automatically detected the center of the optic disc and extracted a 3.46-mm-diameter peripapillary circle to calculate RNFL thickness at each point of the circle. Four-quadrant thickness and global 360° average thickness provided by Cirrus OCT were used in the study, and the correlation between GCIPL and papillary RNFL thicknesses was analyzed.

CFT and GCIPLT were classified into 3 grades according to the statistical percentile (33.3% and 66.6%). EZ appearance in the OCT images was graded from 1 to 3 as follows: Grade 1, shortened EZ (obtained from cross-section of 6 mm horizontal and vertical scans) more than 1 mm; Grade 2, shortened EZ less than 1 mm; and Grade 3, EZ not visible.

2.3. Statistical analysis

Statistical analysis was performed with the Statistical Package for the Social Sciences (SPSS) for Windows (version 20.0; SPSS Inc.; Chicago, IL). Photographs were made using SPSS 20.0 and Graph Pad Prism5 software (Graph Pad Software, Inc., La Jolla, CA). Differences between the RP patients and the normal controls were tested with the Mann–Whitney *U* test and the Kruskal–Wallis test. Associations between the various OCT parameters and BCVA were examined using Spearman rank correlation. All factors affecting visual acuity were analyzed further by multiple linear regressions. Criterion significance was assessed at the $P < 0.05$ level.

3. Results

Seventy eyes of 35 RP patients and 65 eyes without retinal diseases were enrolled in the study. One eye with unacceptable GCIPL OCT image and 1 eye with an unreliable papillary RNFL OCT image were excluded in RP group, so there were 68 eyes analyzed in the study. There were no statistically significant differences in age or gender between the RP patients and the normal controls.

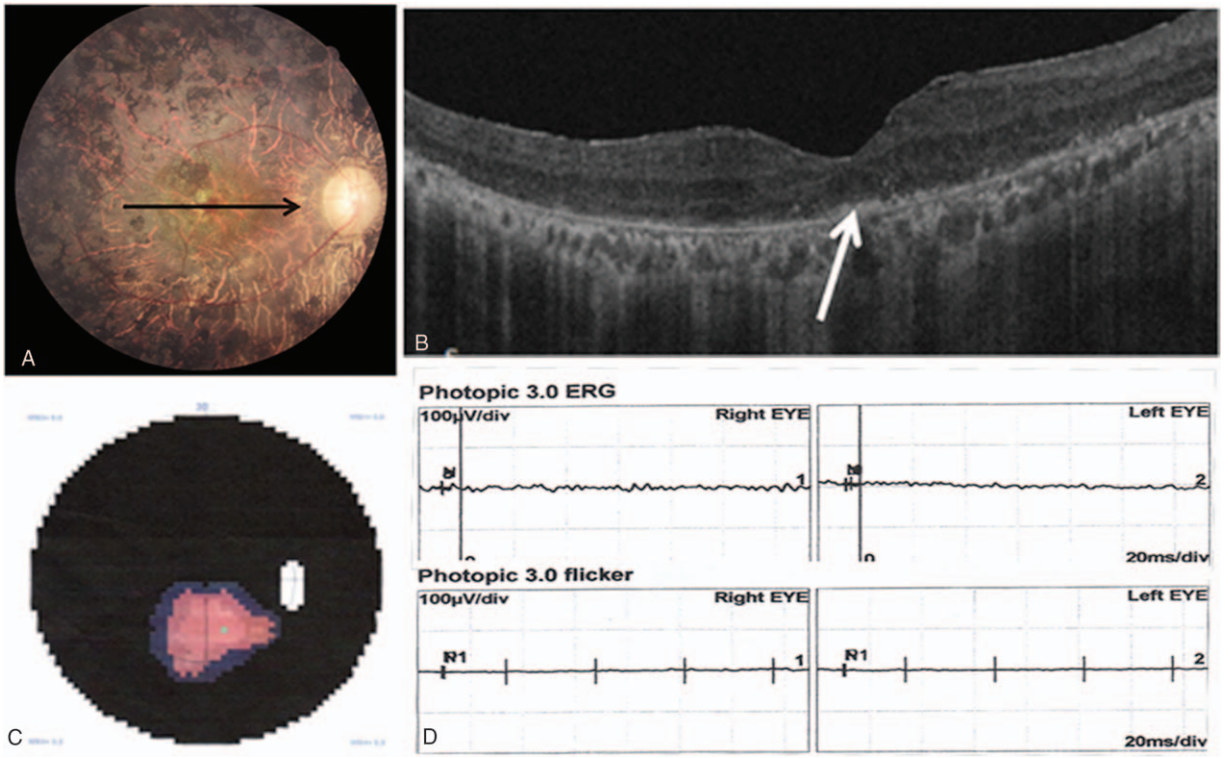

Figure 1. Characteristics of retinitis pigmentosa. (A) Fundus photograph with a black line (arrow) indicates the direction of the horizontal scan. (B) A shortened ellipsoid zone (white arrow) can be seen; the best corrected visual acuity was 0.5. (C) The extent of the visual field was less than 15°. (D) Electroretinography responses were almost nonrecordable.

3.1. Characteristics of RP

As shown in Fig. 1, the typical fundus changes in RP patients include bone spicule-shaped pigment deposits, attenuation of the retinal vessels, waxy pallor of the optic disc, and various degrees of retinal atrophy. A disrupted EZ, concentric constriction of the visual field, and nonrecordable ERG responses are found in the late stage of RP.

3.2. Analysis of retinal thickness in macular area

The macular thickness analysis, including the central subfield, outer ring, area thickness, and posterior pole retinal volume are listed in Table 1. CFT and area macular thickness were 216.2 ± 66.7 and 239.2 ± 32.4 μm in the RP patients, respectively, and in the control group were 245.2 ± 22.4 and 283.0 ± 14.0 μm. Posterior pole retinal volume was 8.6 ± 1.2 mm^3 in the RP patients, while in control group was 10.2 ± 0.5 mm^3. These values were significantly lower in RP patients ($P < 0.001$).

3.3. Thickness map and macular retinal ganglion cell–inner plexiform layer thickness

As shown in Fig. 2, the images showed the retinal GCIPLT map, and the OCT parameter was measured in 6 sectors. Representative case of normal subject (left eye of 50-year-old male) (Fig. 2A). Representative case of RP patient (left eye of 54-year-old male) (Fig. 2B). The images showed that RP patients had thinner GCIPL thickness than normal controls in 6 sectors. The original data of

Table 1

Comparison of macular thickness and volume between RP patients and normal controls.

Parameter	RP group			Control group			t	P
	Mean ± standard deviation	Range	95% Confidence interval	Mean ± standard deviation	Range	95% Confidence interval		
Macular thickness analysis, macular cube								
Central foveal thickness, μm	216.2 ± 66.7	89.0–434.0	200.3–232.0	245.2 ± 22.4	199.0–295.0	239.6–250.7	−3.593	<0.001
Superior retinal thickness, μm	241.4 ± 28.0	168.0–303.0	234.7–248.0	285.0 ± 19.5	179.0–319.0	280.1–289.9	−7.934	<0.001
Temporal retinal thickness, μm	231.2 ± 33.2	185.0–360.0	223.3–239.1	269.4 ± 15.1	239.0–315.0	265.7–273.2	−7.984	<0.001
Inferior retinal thickness, μm	239.4 ± 30.7	178.0–307.0	232.1–246.7	273.1 ± 14.3	246.0–320.0	269.5–276.7	−6.738	<0.001
Nasal retinal thickness, μm	263.7 ± 37.5	155.0–340.0	254.7–272.6	303.4 ± 17.8	254.0–349.0	298.9–307.8	−6.729	<0.001
6 × 6 square area retinal thickness, μm	239.2 ± 32.4	159.0–311.0	231.4–246.9	283.0 ± 14.0	230.0–318.0	279.5–286.4	−7.734	<0.001
6 × 6 square area retinal volume, mm^3	8.6 ± 1.2	5.7–11.2	8.3–8.9	10.2 ± 0.5	8.3–11.5	10.2–10.1	−7.707	<0.001

RP = retinitis pigmentosa.

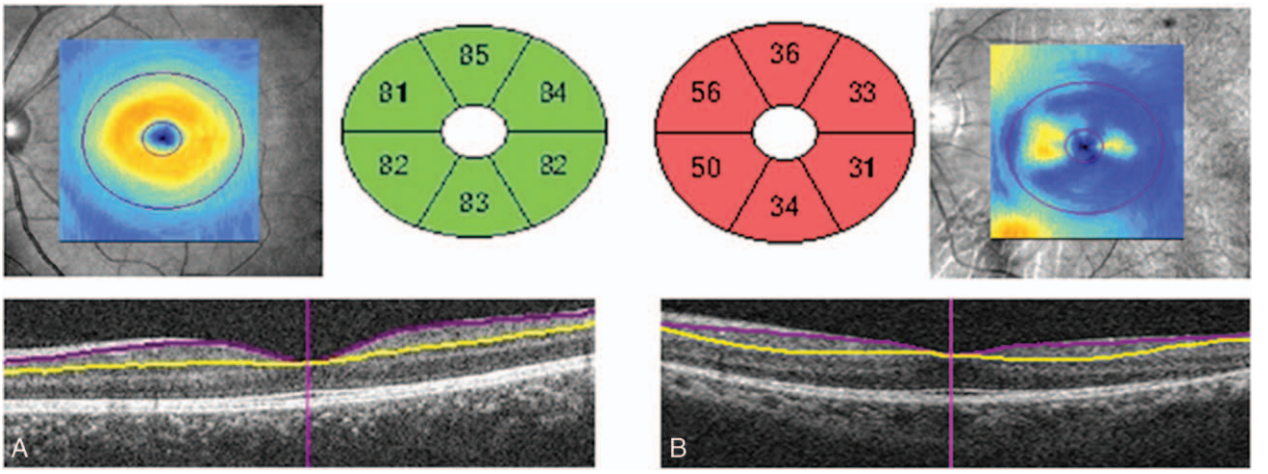

Figure 2. Thickness map and macular retinal ganglion cell–inner plexiform layer (GCIPL) thickness. The ganglion cell analysis algorithm identifies the outer boundaries of retinal nerve fiber layer and inner plexiform layer, between which is the GCIPL layer. (A) Representative case of normal subject (left eye of 50-year-old male). (B) Representative case of retinitis pigmentosa (RP) patient (left eye of 54-year-old male). The images showed that RP patients had thinner GCIPL thickness compared with normal controls in 6 sectors.

GCIPLT in RP patients are shown in Supplementary material, http://links.lww.com/MD/B487.

3.4. Analysis of GCIPLT and ORT in macular area

GCIPLT was measured in 6 different locations: superior, superotemporal, inferotemporal, inferior, inferonasal, and superonasal (Fig. 3A). The mean GCIPLT was $54.7 \pm 18.9\,\mu m$ in the RP patients and $85.6 \pm 6.8\,\mu m$ in the normal controls (Table 2). GCIPLT in all quadrants became thinner significantly ($P < 0.001$), especially in the temporal area (Fig. 3B). Detailed GCIPLT data in the different quadrants are presented in Table 2. The corresponding ORT was classified into 3 grades according to the statistical percentile (33.3% and 66.6%) of GCIPLT: 43.1, 73.3, and $101.4\,\mu m$, respectively. The GCIPLT thinning was consistent with the ORT thinning ($P < 0.001$). The correlation between GCIPLT and ORT was significant when evaluated with a linear regression model ($r = 0.436$, $P < 0.001$).

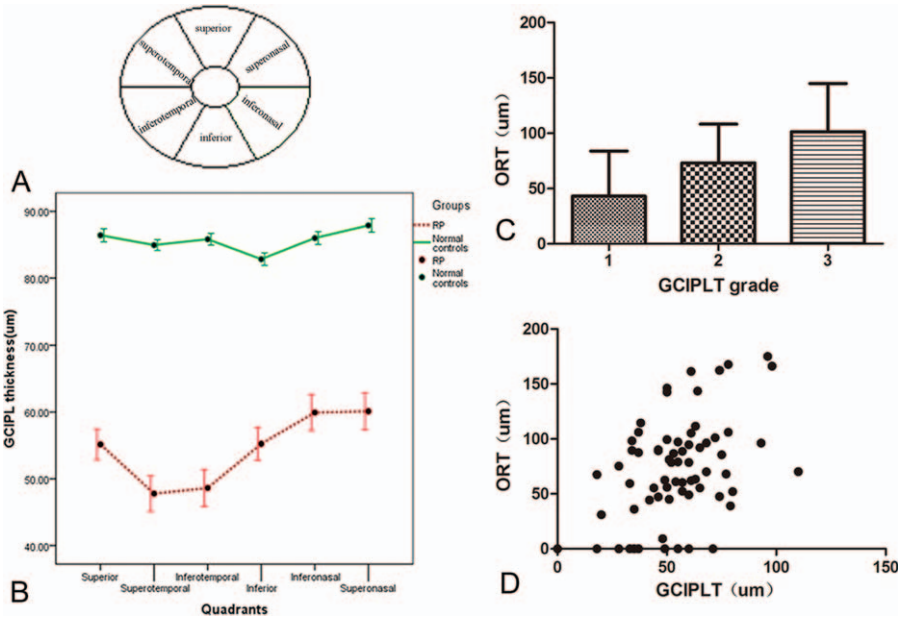

Figure 3. Ganglion cell–inner plexiform layer thickness (GCIPLT) and outer retinal thickness (ORT) measurements. (A) Representative optical coherence tomography image of a right eye in 6 sectors (superonasal, superior, superotemporal, inferotemporal, inferior, and inferonasal). (B) GCIPL thickness was measured using the Cirrus linear measurement tool at 6 locations. Compared with healthy eyes, the thickness of the ganglion cell–plexiform layer in various quadrants was significantly thinner in retinitis pigmentosa patients. ORT was defined as a region from the outer plexiform layer to the retinal pigment epithelium layer/Bruch complex. The thickness of the outer retina was classified into 3 grades according to the statistical percentile (33.3% and 66.6%) of GCIPLT. (C) The results showed that the thinning of GCIPLT was coincident with the thinning of ORT ($P < 0.001$). (D) The correlation between GCIPLT and ORT was significant when evaluated by a linear regression model ($r = 0.436$, $P < 0.001$).

Table 2

Comparison of GCIPLT between RP patients and normal controls.

Parameter	RP group			Control group			t	P
	Mean ± standard deviation	Range	95% Confidence interval	Mean ± standard deviation	Range	95% Confidence interval		
GCIPL, μm								
Average	54.7 ± 18.9	18.0–110.0	50.2–59.2	85.6 ± 6.8	70.0–103.0	83.8–87.3	−8.579	<0.001
Minimum	32.6 ± 21.2	0.0–97.0	27.5–37	81.5 ± 9.3	43.0–101.0	79.2–83.9	−8.923	<0.001
Superior	55.1 ± 19.1	13.0–108.0	50.6–59.7	86.4 ± 7.8	71.0–103.0	84.4–88.4	−8.476	<0.001
Superotemporal	47.8 ± 22.1	7.0–107.0	42.5–53.1	85.0 ± 6.4	74.0–101.0	83.3–86.6	−8.111	<0.001
Inferotemporal	48.6 ± 22.8	0.0–102.0	43.1–54.1	85.8 ± 6.9	71.0–105.0	84.1–87.6	−7.839	<0.001
Inferior	55.0 ± 20.6	14.0–110.0	50.0–60.0	82.8 ± 7.4	57.0–98.0	81.0–84.7	−7.757	<0.001
Inferonasal	60.1 ± 22.2	11.0–111.0	54.8–65.5	86.0 ± 7.6	69.0–105.0	84.1–87.9	−7.543	<0.001
Superonasal	60.1 ± 23.0	8.0–126.0	54.6–65.6	87.9 ± 8.1	70.0–107.0	85.9–89.9	−7.741	<0.001

GCIPL = ganglion cell–inner plexiform layer, RP = retinitis pigmentosa.

3.5. Analysis of peripapillary RNFL thickness

The thickness of the peripapillary RNFL in the different quadrants is presented in Table 3. The mean thickness of the peripapillary RNFL was 102.1 ± 24.1 μm in the RP patients and 101.1 ± 10.5 μm in the control group; the difference was not significant. The peripapillary RNFL thicknesses in the superior, inferior, nasal, and temporal quadrants were 113.6 ± 35.8, 117.2 ± 36.7, 83.0 ± 24.8, and 95.6 ± 21.8 μm, respectively, in the RP patients and 124.2 ± 21.0, 134.7 ± 18.8, 71.7 ± 11.0, and 73.7 ± 10.7 μm, respectively, in the control group. Compared with the normal controls, RNFL thicknesses in the RP patients were significantly thicker in the temporal and nasal areas ($P = 0.001$) and thinner in the superior and inferior areas ($P < 0.05$) (Fig. 4).

3.6. Length of EZ and ELM line in RP patients

In the RP patients, the EZ and ELM lines were present in varying lengths at the fovea and absent outside the macula. The lengths of the residual EZ and ELM lines depicted in the OCT images were measured (Fig. 5A), and the average lengths were 911.1 ± 208.8 and 1621.2 ± 233.5 μm, respectively. The length of the ELM line was significantly longer than the average EZ length ($P < 0.005$) (Fig. 5B). The correlation between ELM line length and EZ shortening was strong ($r = 0.862$, $P < 0.001$) (Fig. 5C). The original data of EZ length in RP patients are shown in Supplementary material, http://links.lww.com/MD/B487.

3.7. Correlations between BCVA and CFT, GCIPLT, and EZ length

CFT and GCIPLT were classified into 3 grades according to the statistical percentile (33.3% and 66.6%). The length of the EZ in the OCT images was graded from 1 to 3, as follows: Grade 1, average EZ greater than 1 mm, and the longest EZ was less than 3 mm; Grade 2, abnormal EZ less than 1 mm; and Grade 3, EZ not visible. As shown in Fig. 6A1–C1, RP patients with a thicker CFT, GCIPLT and longer EZ had better BCVA ($P < 0.001$). The results of an evaluation using a linear regression model showed that there was a significant positive correlation between BCVA and CFT ($r = -0.5933$, $P < 0.001$), GCIPLT ($r = -0.452$, $P < 0.001$), and EZ length ($r = -0.7622$, $P < 0.001$) (Fig. 6A2–C2); the EZ at the fovea demonstrated the strongest relationship with BCVA followed by GCIPLT and CFT. All of the factors affecting visual acuity were further analyzed by multiple linear regressions. Regression coefficients for significant factors are compared in Table 4. The results show that CFT (Beta [B] = −0.286; $P = 0.014$), GCIPLT (Beta [B] = −0.217; $P = 0.047$), and EZ length (Beta [B] = −0.311; $P = 0.013$) were associated significantly with BCVA.

4. Discussion

In this study, we aimed to investigate the changes in retinal photoreceptor EZ and postreceptor retinal layer in RP patients by GCA and analyze the relationship between the OCT parameters and BCVA. First, we examined CFT, and the results showed that the RP patients had significant thinning of CFT compared with the controls. The RP patients with thicker CFT had better BCVA, so there was a positive correlation between CFT and BCVA, which was consistent with the previous studies.[15,28]

The earliest histopathological changes in all forms of RP involve shortening of the photoreceptor segments, but there are fewer articles about inner retinal thickness. The previous study reported that the inner nuclear, inner plexiform, and retinal

Table 3

Comparison of RNFL thicknesses between RP patients and normal controls.

Parameter	RP group			Control group			t	P
	Mean ± standard deviation	Range	95% Confidence interval	Mean ± standard deviation	Range	95% Confidence interval		
RNFL thickness, μm								
Mean	102.1 ± 24.1	61.0–165.0	96.3–107.9	101.1 ± 10.5	83.0–128.0	98.4–103.8	−0.148	0.882
Superior	113.6 ± 35.8	7.0–197.0	105.1–122.1	124.2 ± 21.0	72.0–174.0	118.9–129.5	−2.091	0.037
Temporal	95.6 ± 21.8	53.0–158.0	90.4–100.8	73.7 ± 10.7	52.0–99.0	71.0–76.4	−6.038	<0.001
Inferior	117.2 ± 36.7	43.0–205.0	108.5–126.0	134.7 ± 18.8	100.0–197.0	130.0–139.5	−3.340	0.001
Nasal	83.0 ± 24.8	40.0–217.0	77.0–88.9	71.7 ± 11.0	48.0–94.0	68.9–74.5	−3.230	0.001

RNFL = retinal nerve fiber layer, RP = retinitis pigmentosa.

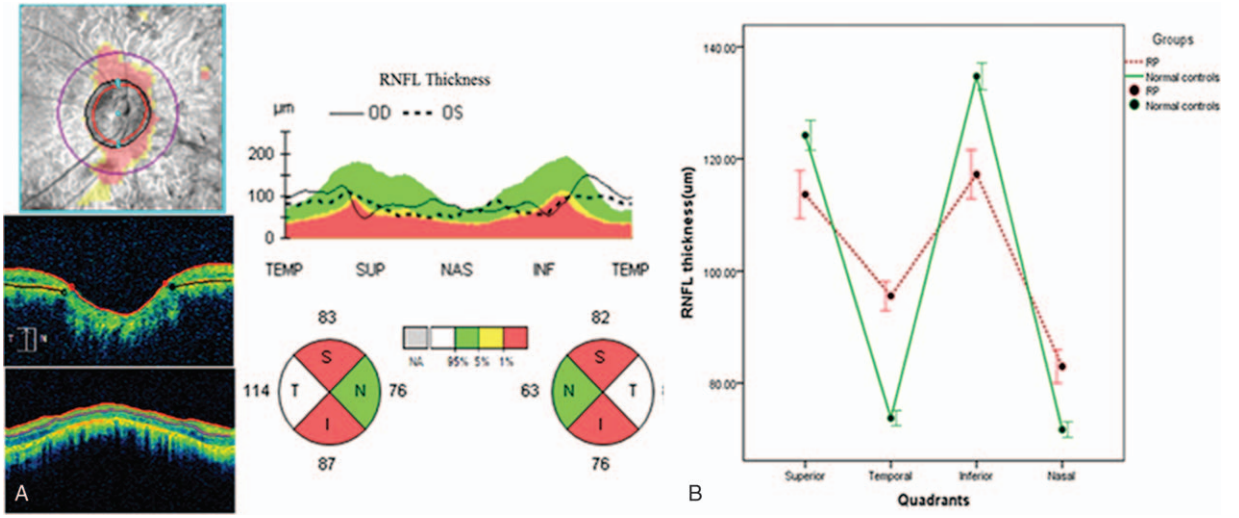

Figure 4. Peripapillary retinal nerve fiber layer (RNFL) thickness measurements. (A) Representative papillary optical coherence tomography image of a right eye in retinitis pigmentosa (RP) patient with RNFL thickness map and RNFL thickness values in different regions. (B)The results showed that peripapillary RNFL thicknesses did not differ significantly between the RP and control groups, but in the temporal and nasal quadrants, the RP group had a significantly thicker RNFL, while RNFL thinning was seen in the superior and inferior areas. However, total RNFL thickness was greater in the superior and inferior areas than in the temporal and nasal areas.

GCLs were relatively intact.[11] In addition, the clinical and morphometry studies showed the similar results that inner retinal layers were preserved in the RP groups.[10,13] What is more, even inner retinal thickening was detected, which was related with neuronal–glial remodeling response to photoreceptor loss in RP patients,[29,30] but the patients in later stage with decreased inner retinal thickness was also proved.[12] In addition, the histopathologic studies reported that RP had significantly fewer ganglion cells than those of the control group,[14] and the thickness of GCL combined IPL was significantly thinner in RP by OCT.[15] In addition, the new articles showed that ganglion cells decreased because of inherited photoreceptor degeneration in animal studies,[31,32] which was related with deficit of the retrograde axonal transport lead by inherited photoreceptor degeneration.[33] Therefore, in the present study, we used GCA as a new method for assessing the structural changes of GCIPL, which is related to the photoreceptor degeneration in RP patients. Compared with the measurement in previous studies, GCA assesses the thickness by a macular cube 512×128 scan from more sites; as a result, we can obtain more detail and accurate GCIPLT data by the GCA combined with the modern OCT device with an axial resolution of 5 μm. Our results showed that GCIPLT in all quadrants exhibited significant thinning and that the thinning was greater in the superior and temporal quadrants than in the nasal and inferior quadrants, which indicated that the RP patients had decreased retinal thickness both in outer retina and inner retina in our study.

While the thinning of ORT has been known, whether there is a relationship between GCIPLT and ORT has not been reported in RP patients. In the present study, we assessed the correlation

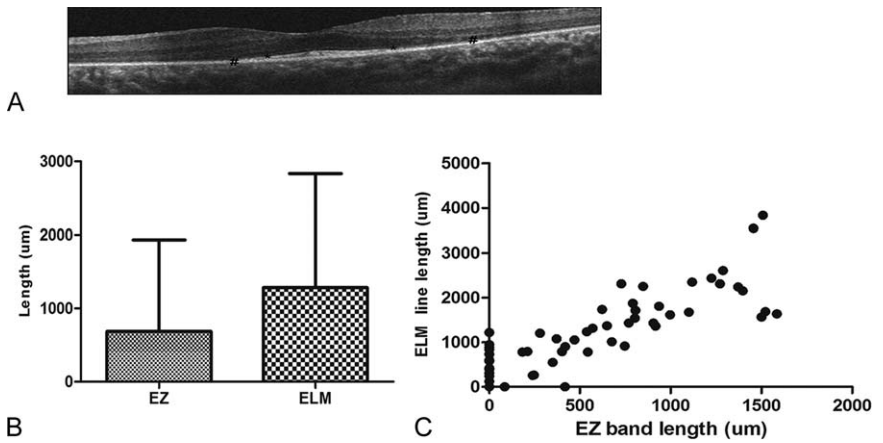

Figure 5. Ellipsoid zone (EZ) and extend limiting membrane (ELM) line. Grayscale images were used for the measurement of the EZ and ELM. Length was measured in the horizontal and vertical scans, and an average value was obtained. (A) The disrupted photoreceptor EZ (*) and ELM (#) can be seen in the optical coherence tomography imagine. (B) Mean lengths of the EZ and ELM lines in 68 eyes with retinitis pigmentosa. ELM length was significantly greater than EZ length ($P < 0.005$, $t = -3.107$). (C) There is a significant positive correlation between the lengths of the EZ and ELM lines ($r = 0.862$, $P < 0.001$).

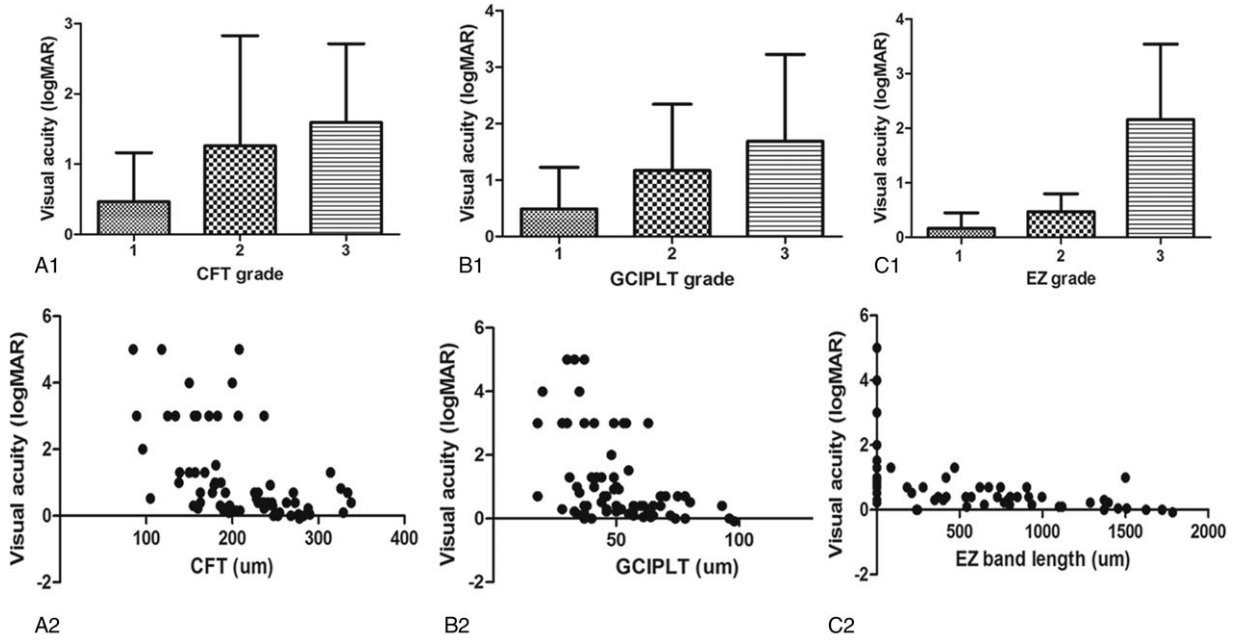

Figure 6. Relationship between best corrected visual acuity (BCVA) and central fovea thicknesses (CFT), ganglion cell–inner plexiform layer thickness (GCIPLT), and ellipsoid zone (EZ). CFT and GCIPLT were graded from 1 to 3 according to statistical percentile (33.3% and 66.6%). The appearance of the EZ in the optical coherence tomography (OCT) images was graded from 1 to 3: Grade 1, shortened EZ greater than 1 mm; Grade 2, shortened EZ less than 1 mm; and Grade 3, EZ not visible. Mean visual acuity (log MAR units) as a function of the grade of the OCT parameters. (A1–C1) The difference among the 3 groups was statistically significant ($P < 0.005$). Retinitis pigmentosa patients with thicker CFT and GCIPLT and longer EZ had better BCVA ($P < 0.001$). (A2–C2) The correlations among BCVA and CFT, GCIPLT, and EZ were evaluated using a linear regression model. The results showed significant positive correlations among BCVA and CFT ($r = -0.5933$, $P < 0.001$), GCIPLT ($r = -0.452$, $P < 0.001$), and EZ ($r = -0.7622$, $P < 0.001$); EZ at the fovea demonstrated a stronger relationship with BCVA.

between GCIPLT and ORT, and the results showed that GCIPLT thinning was significantly related to the decreased ORT as well as the macular retinal thickness. We further assessed the correlation between GCIPLT and BCVA, RP patients with thicker GCIPLT had better BCVA, but the correlation was moderate. The reasons might be that some eyes with poor visual acuity still preserved the thickness of the RGC, and the present OCT could not distinguish the transition between the GCL and the IPL. So a larger study cohort and new OCT with a more precise segmentation of the retinal layers is needed in the future study. To summarize, the inner retina might be relative preserved in the early stage of RP; the thickness was decreased with the progression of the disease, especially in the late stage and advanced ones.

RNFL is the axon originating from the ganglion cells, so we measured the thickness to see whether the papillary RNFL thinning occurred along with the degeneration of ganglion cell. In the previous studies, the changes in RNFL thickness are inconsistent, including thickening, thinning, or relative uniformity, measured by time domain OCT or spectral domain OCT.[34–38] In addition, the relevant studies have indicated that RNFL thickening was most common in the temporal area, and RNFL thinning was found in the nasal and inferior regions.[35,37] However, results in our study showed that the average papillary RNFL thickness did not change significantly compared with the normal controls. But there existed a spatial preference of RNFL thickening in the temporal and nasal directions and RNFL thinning in the inferior and superior areas. These findings suggest that RNFL thickness changed in the RP eyes along with the degeneration of ganglion cell. But the reasons accounting for RNFL thickening or thinning in different areas need to be investigated in further researches.

Although the mechanism of RNFL degeneration is different from glaucoma, the orders of RNFL thinning are similar in the sequence of RNFL thinning.[39] A recent study reported that compromised axonal transport would lead to RGC loss and decreased RNFL thickness during the developing process of RP,

Table 4

Multivariate logistic regression analysis of different factors significantly affecting BCVA.

	Unstandardized coefficients		Standardized coefficients		
Model	**B**	**SE**	**Beta (B)**	**t**	***P***
(Constant)	3.679	0.586		6.275	0.000
CFT	−006	0.003	−286	−2.517	0.014
GCIPLT	−017	0.008	−217	−2.024	0.047
EZ band	−001	0.000	−311	−2.547	0.013

BCVA = best corrected visual acuity, CFT = central foveal thickness, EZ = ellipsoid zone, GCIPLT = ganglion cell–inner plexiform layer thickness.

and the maximum transneuronal damage occurred mainly in the inferonasal quadrant,[35] which was consistent with the results in our study. Apart from RNFL thinning, the reasons for RNFL thickening have been studied, it has been reported that with the progress of RNFL degeneration, the proliferative glial cell displacing the atrophic nerve fiber and edematous changes of the residual RNFL were attributed to a thickened RNFL.[34] Hood et al[11] speculated that a purely mechanical factor compelling the thickening RNFL partially filled the quadrants where the receptors degenerated. As a result, RNFL thickening is found in the area where GCIPL thinning is greatest in RP patients. So while the regions of GCIPL thinning are corresponded to the areas of RNFL defects in glaucoma,[40] it is almost the opposite in RP patients. The results suggest that it should be prudent to make optimal use of RNFL thickness for predicting the status of RGC in patients with RP. Refer to the discrepancies among the different studies, it might stem from differences in OCT devices and the discordant stages of RP in the study populations.

With the progression of RP, EZ disappeared from the peripheral part toward the fovea on the OCT images. Therefore, measuring the length of the residual EZ in RP patients is very useful for estimating residual central visual function. According to the length of the EZ, RP patients in our study were graded into 3 groups: Grade 1, shortened EZ greater than 1 mm; Grade 2, shortened EZ less than 1 mm; and Grade 3, EZ not visible. The relationship between BCVA and EZ was significant, which is agreed with the results in the previous studies.[41,42] Thus, the average length of the EZ is an important OCT parameter for monitoring visual acuity in RP patients.

With regard to the outer hyperreflected lines, the ELM line was found to be longer than the EZ. Pathological studies about RP confirmed that the earliest histopathological change is in the outer segments of photoreceptors,[9] where EZ is located. In addition, ELM consists of photoreceptor inner segment and Müller cell processes,[43] so EZ became disorganized earlier than ELM, but the shortened ELM lines were significantly related with EZ defect.

Taken together, GCA is a new method to measure the GCIPLT, which helps to prove the real changes in the inner retinal layers of RP patients. Our further results showed that postreceptor retinal layer (GCIPLT) became significantly thinner along with the retinal photoreceptor EZ degeneration in all quarter, which was correlated with BCVA in RP patients. So, we assess retinal layer changes with the advent of the GCA software combined with the modern OCT devices from a new perspective and to quantify the changes both in outer and inner retinal layers, which are very useful for diagnosis, staging, and prognosis of RP.

References

[1] Daiger SP, Sullivan LS, Bowne SJ. Genes and mutations causing retinitis pigmentosa. Clin Genet 2013;84:132–41.

[2] Hartong DT, Berson EL, Dryja TP. Retinitis pigmentosa. Lancet 2006;368:1795–809.

[3] Daiger SP, Bowne SJ, Sullivan LS. Genes and mutations causing autosomal dominant retinitis pigmentosa. Cold Spring Harb Perspect Med 2014;10:5.

[4] Haim M. Epidemiology of retinitis pigmentosa in Denmark. Acta Ophthalmol Scand Suppl 2002;233:1–34.

[5] Fariss RN, Li ZY, Milam AH. Abnormalities in rod photoreceptors, amacrine cells, and horizontal cells in human retinas with retinitis pigmentosa. Am J Ophthalmol 2000;129:215–23.

[6] Szamier RB, Berson EL, Klein R, et al. Sex-linked retinitis pigmentosa: ultrastructure of photoreceptors and pigment epithelium. Invest Ophthalmol Vis Sci 1979;18:145–60.

[7] Hood DC, Lazow MA, Locke KG, et al. The transition zone between healthy and diseased retina in patients with retinitis pigmentosa. Invest Ophthalmol Vis Sci 2011;52:101–8.

[8] Hood DC, Ramachandran R, Holopigian K, et al. Method for deriving visual field boundaries from oct scans of patients with retinitis pigmentosa. Biomed Opt Express 2011;2:1106–14.

[9] Milam AH, Li ZY, Fariss RN. Histopathology of the human retina in retinitis pigmentosa. Prog Retin Eye Res 1998;17:175–205.

[10] Santos A, Humayun MS, de Juan EJr, et al. Preservation of the inner retina in retinitis pigmentosa. A morphometric analysis. Arch Ophthalmol 1997;115:511–5.

[11] Hood DC, Lin CE, Lazow MA, et al. Thickness of receptor and postreceptor retinal layers in patients with retinitis pigmentosa measured with frequency-domain optical coherence tomography. Invest Ophthalmol Vis Sci 2009;50:2328–36.

[12] Aleman TS, Cideciyan AV, Sumaroka A, et al. Inner retinal abnormalities in X-linked retinitis pigmentosa with RPGR mutations. Invest Ophthalmol Vis Sci 2007;48:4759–65.

[13] Humayun MS, Prince M, de Juan EJr, et al. Morphometric analysis of the extramacular retina from postmortem eyes with retinitis pigmentosa. Invest Ophthalmol Vis Sci 1999;40:143–8.

[14] Stone JL, Barlow WE, Humayun MS, et al. Morphometric analysis of macular photoreceptors and ganglion cells in retinas with retinitis pigmentosa. Arch Ophthalmol 1992;110:1634–9.

[15] Vamos R, Tatrai E, Nemeth J, et al. The structure and function of the macula in patients with advanced retinitis pigmentosa. Invest Ophthalmol Vis Sci 2011;52:8425–32.

[16] Nakatani Y, Higashide T, Ohkubo S, et al. Influences of the inner retinal sublayers and analytical areas in macular scans by spectral-domain OCT on the diagnostic ability of early glaucoma. Invest Ophthalmol Vis Sci 2014;55:7479–85.

[17] Curcio CA, Allen KA. Topography of ganglion cells in human retina. J Comp Neurol 1990;300:5–25.

[18] Kim MJ, Park KH, Yoo BW, et al. Comparison of macular GCIPL and peripapillary RNFL deviation maps for detection of glaucomatous eye with localized RNFL defect. Acta Ophthalmol 2015;93:e22–8.

[19] Mwanza JC, Budenz DL, Godfrey DG, et al. Diagnostic performance of optical coherence tomography ganglion cell–inner plexiform layer thickness measurements in early glaucoma. Ophthalmology 2014;121:849–54.

[20] Sieving PA, Caruso RC, Tao W, et al. Ciliary neurotrophic factor (CNTF) for human retinal degeneration: phase I trial of CNTF delivered by encapsulated cell intraocular implants. Proc Natl Acad Sci U S A 2006;103:3896–901.

[21] Jensen RJ, Rizzo JF. Activation of retinal ganglion cells in wild-type and rd1 mice through electrical stimulation of the retinal neural network. Vision Res 2008;48:1562–8.

[22] Yokochi M, Li D, Horiguchi M, et al. Inverse pattern of photoreceptor abnormalities in retinitis pigmentosa and cone-rod dystrophy. Doc Ophthalmol 2012;125:211–8.

[23] Sugita T, Kondo M, Piao CH, et al. Correlation between macular volume and focal macular electroretinogram in patients with retinitis pigmentosa. Invest Ophthalmol Vis Sci 2008;49:3551–8.

[24] Apushkin MA, Fishman GA, Alexander KR, et al. Retinal thickness and visual thresholds measured in patients with retinitis pigmentosa. Retina 2007;27:349–57.

[25] Oishi A, Nakamura H, Tatsumi I, et al. Optical coherence tomographic pattern and focal electroretinogram in patients with retinitis pigmentosa. Eye (London) 2009;23:299–303.

[26] Mwanza JC, Oakley JD, Budenz DL, et al. Macular ganglion cell–inner plexiform layer: automated detection and thickness reproducibility with spectral domain-optical coherence tomography in glaucoma. Invest Ophthalmol Vis Sci 2011;52:8323–9.

[27] Mwanza JC, Durbin MK, Budenz DL, et al. Glaucoma diagnostic accuracy of ganglion cell–inner plexiform layer thickness: comparison with nerve fiber layer and optic nerve head. Ophthalmology 2012;119:1151–8.

[28] Tamaki M, Matsuo T. Optical coherence tomographic parameters as objective signs for visual acuity in patients with retinitis pigmentosa, future candidates for retinal prostheses. J Artif Organs 2011;14:140–50.

[29] Krishnamoorthy V, Cherukuri P, Poria D, et al. Retinal remodeling: concerns, emerging remedies and future prospects. Front Cell Neurosci 2016;10:38.

[30] Beltran WA, Hammond P, Acland GM, et al. A frameshift mutation in RPGR exon ORF15 causes photoreceptor degeneration and inner retina remodeling in a model of X-linked retinitis pigmentosa. Invest Ophthalmol Vis Sci 2006;47:1669–81.

[31] Anderson EE, Greferath U, Fletcher EL. Changes in morphology of retinal ganglion cells with eccentricity in retinal degeneration. Cell Tissue Res 2016;364:263–71.
[32] Garcia-Ayuso D, Di Pierdomenico J, Esquiva G, et al. Inherited photoreceptor degeneration causes the death of melanopsin-positive retinal ganglion cells and increases their coexpression of Brn3a. Invest Ophthalmol Vis Sci 2015;56:4592–604.
[33] García-Ayuso D, Salinas-Navarro M, Nadal-Nicolás FM, et al. Sectorial loss of retinal ganglion cells in inherited photoreceptor degeneration is due to rgc death. Br J Ophthalmol 2014;98:396–401.
[34] Oishi A, Otani A, Sasahara M, et al. Retinal nerve fiber layer thickness in patients with retinitis pigmentosa. Eye (London) 2009;23:561–6.
[35] Walia S, Fishman GA. Retinal nerve fiber layer analysis in RP patients using Fourier-domain OCT. Invest Ophthalmol Vis Sci 2008;49:3525–8.
[36] Walia S, Fishman GA, Edward DP, et al. Retinal nerve fiber layer defects in RP patients. Invest Ophthalmol Vis Sci 2007;48:4748–52.
[37] Anastasakis A, Genead MA, McAnany JJ, et al. Evaluation of retinal nerve fiber layer thickness in patients with retinitis pigmentosa using spectral-domain optical coherence tomography. Retina 2012;32:358–63.
[38] Xue K, Wang M, Chen J, et al. Retinal nerve fiber layer analysis with scanning laser polarimetry and RTVue-OCT in patients of retinitis pigmentosa. Ophthalmologica 2013;229:38–42.
[39] Medeiros FA, Zangwill LM, Alencar LM, et al. Detection of glaucoma progression with stratus OCT retinal nerve fiber layer, optic nerve head, and macular thickness measurements. Invest Ophthalmol Vis Sci 2009;50:5741–8.
[40] Kim KE, Park KH, Jeoung JW, et al. Severity-dependent association between ganglion cell–inner plexiform layer thickness and macular mean sensitivity in open-angle glaucoma. Acta ophthalmol 2014;92:e650–6.
[41] Aizawa S, Mitamura Y, Baba T, et al. Correlation between visual function and photoreceptor inner/outer segment junction in patients with retinitis pigmentosa. Eye (London) 2009;23:304–8.
[42] Mitamura Y, Mitamura-Aizawa S, Katome T, et al. Photoreceptor impairment and restoration on optical coherence tomographic image. J Ophthalmol 2013;2013:518170.
[43] Gloesmann M, Hermann B, Schubert C, et al. Histologic correlation of pig retina radial stratification with ultrahigh-resolution optical coherence tomography. Invest Ophthalmol Vis Sci 2003;44:1696–703.